Supporting Information

Single-Crystal-to-Single-Crystal Transformation and Proton Conductivity of Three Hydrogen-Bonded Organic Frameworks

Yijie Wang ,[a] Zhang minghui,[a] Qianqian Yang,[a] Jianbo Yin,[a] Di Liu,[a] Yanxue Shang,[a] Zixi, Kang,[b] Rongming Wang,[a,b,*] Daofeng Sun[a,b] and Jianzhuang Jiang,[a,c,*]

[a]College of Science, China University of Petroleum (East China), Qingdao Shandong 266580, China.
[b]State Key Laboratory of Heavy Oil Processing, School of Materials Science and Engineering, China University of Petroleum (East China), Qingdao Shandong 266580,China.
[c]Beijing Key Laboratory for Science and Application of Functional Molecular and Crystalline Materials, Department of Chemistry, University of Science and Technology Beijing, Beijing 100083, China.

*Corresponding authors: Rongming Wang: (rmwang@upc.edu.cn); Jianzhuang Jiang: (jianzhuang@ustb.edu.cn.)

Materials and Physical Measurements.

4,4'-diaminostilbene-2,2'-disulfonic acid (DAS) (98%, Sahn Chemical Technology (Shanghai) Co., Ltd.), tetramethylammonium hydroxide (TAM) (99%, Sahn Chemical Technology (Shanghai) Co., Ltd.), N,N-Dimethylformamide (>99.5%, Tianjin Fuyu Fine Chemical Co., Ltd), ethanol (> 99.7%, Tianjin Fuyu Fine Chemical Co., Ltd) are reagent grade quality, all are commercial sources, not further purified. The data of powder X-ray diffraction (PXRD) were recorded on an X-Pert PRO MPD diffractometer with Cu-Kα radiation (λ = 0.154178 nm). Thermal gravimetric analysis (TGA) was proceeded on a Mettler Toledo TGA instrument in the range of 40-900 ºC with a heating rate of 10 ºC min-1 under N_2 atmosphere (100 mL min^{-1}). Infrared (IR) spectra were obtained on a Nicolet 330 FTIR spectrometer. Elemental analysis was conducted on a PerkinElmer 240C elemental analyzer for C, H, and N determination.

Synthesis of UPC-H7

4,4'-diamino-2,2'-stilbenedisulfonic acid (5 mg) was dissolved in N,N-Dimethylformamide (5 ml) in a 10 ml glass bottle, and 250 μL of 25 wt% tetramethylammonium hydroxide aqueous solution was added and sonicated for 20 minutes. After sealing, the mixture was heated at 90 °C for 48 hours. The yellow block crystals suitable for single crystal X-ray diffraction analysis were obtained and separated by filtration, then washed using EtOH and dried in air, with a yield of 90%. Elemental analysis calcd (%) for UPC-H7 ($C_{22}H_{36}N_4O_6S_2$): C 51.10, H 6.97, N 11.84; found: C 51.32, H 7.21, N 10.87.

Synthesis of UPC-H8

Single crystals of UPC-H7 (1.00-6.00 mg) in a 3 mL glass vial were placed in an oven and heated at 80 ℃ for 2 hours. The yellow block crystals of UPC-H8 suitable for X-ray

diffraction analysis were obtained. Elemental analysis calcd (%) for UPC-H8 ($C_{22}H_{36}N_4O_6S_2$): C 51.10, H 6.97, N 11.84; found: C 51.68, H 7.02, N 10.88.

Synthesis of UPC-H9

Single crystals of UPC-H8 (1.00-6.00 mg) in a 3 mL glass vial were exposed for 2 hours under 70% R.H. at 80 ℃, then the yellow block crystals of UPC-H9 suitable for X-ray diffraction analysis were obtained. Similarly, Single crystals of UPC-H7 (1.00-6.00 mg) were exposed for 2 hours under 80% R.H. at 40℃, then the yellow block crystals of UPC-H9 suitable for X-ray diffraction analysis were obtained. Elemental analysis calcd (%) for UPC-H9 ($C_{22}H_{40}N_4O_8S_2$): C 47.76, H 7.24, N 10.13; found: C 47.98, H 7.12, N 10.34.

X-ray Crystallography: Single-crystal data of UPC-H7, UPC-H8 and UPC-H9 were collected by an Agilent Super Nova Dual diffractometer using Cu/Kα radiation (λ = 1.54178 Å) at 150 K and focusing multilayer mirror optics. The structures was solved by direct methods using SHELXTL and refined by full-matrix least squares on F2 using SHELX-97. All non-hydrogen atoms were refined with anisotropic displacement parameters during the final cycles. Hydrogen atoms attached to C atoms and amino N atoms were located in calculated positions according to isotropic displacement parameters, and hydrogen atoms attached to O atoms of water molecules were located from the difference electron density maps and refined anisotropically. The crystallographic collection and refinement parameters are listed in Table S1. The crystallographic data was deposited in the Cambridge Crystallographic Data Center (CCDC 1984228 for UPC-H7, CCDC 1984229 for UPC-H8, and CCDC 1984230 for UPC-H9). These data can be obtained free of charge from the CCDC via www.ccdc.cam.ac.uk.

Measurements of proton conductivity.

The pelletized samples for proton conductivity were prepared by the following procedures: The as-synthesized sample of UPC-H7 was placed in a 2.98 mm diameter mold and pressed into a pellet with a thickness of 0.9-1 mm using a tableting machine at 0.5 MPa. The pellet sample was placed in the center of the glass plate and fixed horizontally with two gold wires with a length of about 20 cm, then silver glue is coated to both sides of the pellet sample and waited for about 10 minutes to dry. The single crystal sample for proton conductivity was prepared similar to that of the pelletized sample. The gold wire was carefully attached to the crystal along the opposite surface with conductive silver glue. The proton conduction measurements are taken in three directions of [100], [010], and [001], respectively. The size of the single crystal of UPC-H7 is 0.036 × 0.033 × 0.014 cm^3, 0.032 × 0.028 × 0.013 cm^3 and 0.038 × 0.024 × 0.012 cm^3, respectively. The size of the single crystal of UPC-H9 is 0.037 × 0.033 × 0.023 cm^3, 0.038 × 0.035 × 0.017 cm^3 and 0.039 × 0.027 × 0.012 cm^3, respectively. Impedance analysis was performed with a 1260A Impedance/Gain-Phase Analyzer from 10 MHz to 0.1 Hz with an input voltage 200 mV in a constant temperature and humidity. Humidity and temperature were controlled by using a BPS-50CL humidity control chamber. The impedances at each temperature were measured after equilibration for 30 minutes. The resistance values was obtained by fitting the impedance profile using zview software. The circuit equivalent used for fitting is as follows:

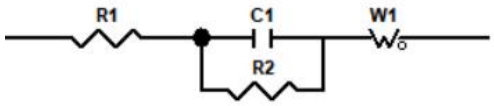

*R*1 corresponds to the resistances of wire and electrode, while *R*2 accounts for the bulk resistance of the pellet.

Proton conductivity was calculated using the following equation:

$$\sigma = \frac{l}{RS}$$

l and *S* are the thickness (cm) and cross-sectional area (cm^2) of the pellet, respectively. *R*

is the bulk resistance of the pellet (*R*2 in the circuit equivalent) fitted by the equivalent circuit of the semicircle in Nyquist plot using zview software. The activation energy (E_a) of the material conductivity is estimated according to the following equation:

$$\sigma T = \sigma_0 exp\ (-\frac{E_a}{k_B T})$$

where σ is the proton conductivity, σ_0 is the pre-exponential factor, k_B is the Boltzmann constant, and T is the temperature.

Table S1. Crystallographic data of UPC-H7, UPC-H8 and UPC-H9**.**

	UPC-H7	UPC-H8	UPC-H9
empirical formula	$C_{22}H_{36}N_4O_6S_2$	$C_{22}H_{36}N_4O_6S_2$	$C_{22}H_{40}N_4O_8S_2$
formula weight	516.67	516.67	552.70
temperature (K)	150	150	150
crystal system	monoclinic	monoclinic	monoclinic
space group	$P2_1/n$	$P2_1/n$	$P2_1/c$
a (Å)	9.7754(3)	9.6616(3)	11.2723(18)
b (Å)	12.5427(4)	12.3127(4)	18.109(3)
c (Å)	22.3714(7)	22.5851(9)	14.821(3)
α (deg)	90	90	90
β (deg)	96.082(3)	97.458(4)	110.51(2)
γ (deg)	90	90	90
volume (Å^3)	2727.52(15)	2664.00(16)	2833.6(9)
Z	4	4	4
ρ_{calc} (g/cm^3)	1.258	1.263	1.380
μ (mm^{-1})	2.120	2.268	2.213
F (000)	1104.0	1012.0	1264.0
GOF on F^2	1.085	1.200	0.914
final R indices [$I > 2\sigma(I)$]	$R_1 = 0.0693$ $wR_2 = 0.1946$	$R_1 = 0.0715$ $wR_2 = 0.1751$	$R_1 = 0.1129$ $wR_2 = 0.2491$

Table S2. Hydrogen Bonding Interactions of UPC-H7[a]

D-H···A	Distance of H···A (Å)	Distance of D···A (Å)	Angle of D-H···A (°)
N1-H1A···O3$^{\#2}$	2.17	2.972(5)	151
N1-H1B···O1$^{\#6}$	2.38	3.236(5)	163
N2-H2A···O2$^{\#4}$	2.44	3.131(5)	136
N2-H2B···O5$^{\#5}$	2.12	2.959(5)	160

[a] Symmetric code, #1: 3/2-x, 1/2+y, 1/2-z, #2: 1/2+x, 3/2-y, 1/2+z, #3: 2-x, 2-y, 1−z, #4: 2-x, 2-y, -z, #5: 5/2-x, 1/2+y, 1/2-z, #6: 3/2-x, 1/2−y, 1/2−z, #7: 3-x, 2−y, 1-z.

Table S3. Hydrogen bonding parameters of UPC-H8[a]

D-H···A	Distance of H···A (Å)	Distance of D···A (Å)	Angle of D-H···A (°)
N1-H1A···O3$^{\#1}$	2.29	3.149(5)	169
N1-H1B···O6$^{\#5}$	2.12	2.960(5)	165
N2-H2A···O1$^{\#4}$	2.09	2.958(6)	179
N2-H2B···O2$^{\#2}$	2.42	3.109(6)	137

[a] Symmetric code, #1: -x, 1-y, 1-z, #2: 1/2-x, 1/2+y, 1/2-z, #3: 1/2+x, 3/2-y, 1/2+z, #4: -1/2+x, 3/2-y, 1/2+z, #5: -1/2+x, 3/2-y, -1/2+z.

Table S4. Hydrogen bonding parameters of UPC-H9[a]

D-H···A	Distance of H···A (Å)	Distance of D···A (Å)	Angle of D-H···A (°)
O2W-H2WA···O2$^{\#4}$	2.33	3.107(17)	151
N1-H1A···O5$^{\#1}$	2.60	3.368(12)	147
N1-H1B···O6	2.67	3.4817(4)	154
O2W-H2WB···O2$^{\#8}$	2.23	3.02(2)	155
N2-H2A···O3$^{\#4}$	2.54	3.223(13)	133
N2-H2B···O5$^{\#7}$	2.44	2.9831(13)	119
O1W-H1WA···N2	2.17	2.87(5)	139
O1W-H1WA···O2W	2.26	2.94(10)	138

[a] Symmetric code, #1: 1+x, 3/2-y, 1/2+z, #2: x, 3/2-y, 1/2+z, #3: -1+x, y, z, #4: -1+x, 3/2-y, -1/2+z, #5: 1-x, 1-y, 1-z, #6: x, 3/2-y, -1/2+z, #7: 1-x, -1/2+y, -1/2-z.

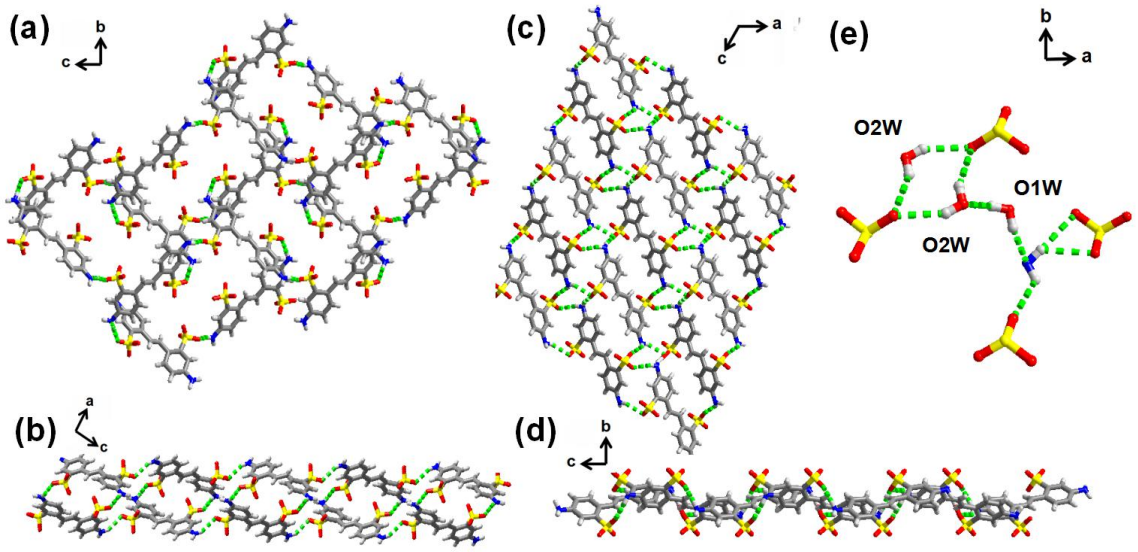

Fig. S1 The 2D hydrogen-bonded network of UPC-H7 viewed along a axis (a) and along b axis (b); the 2D hydrogen-bonded network of UPC-H9 viewed along a axis (c) and along b axis (d); and the hydrogen bonds of water molecules in UPC-H9 (e).

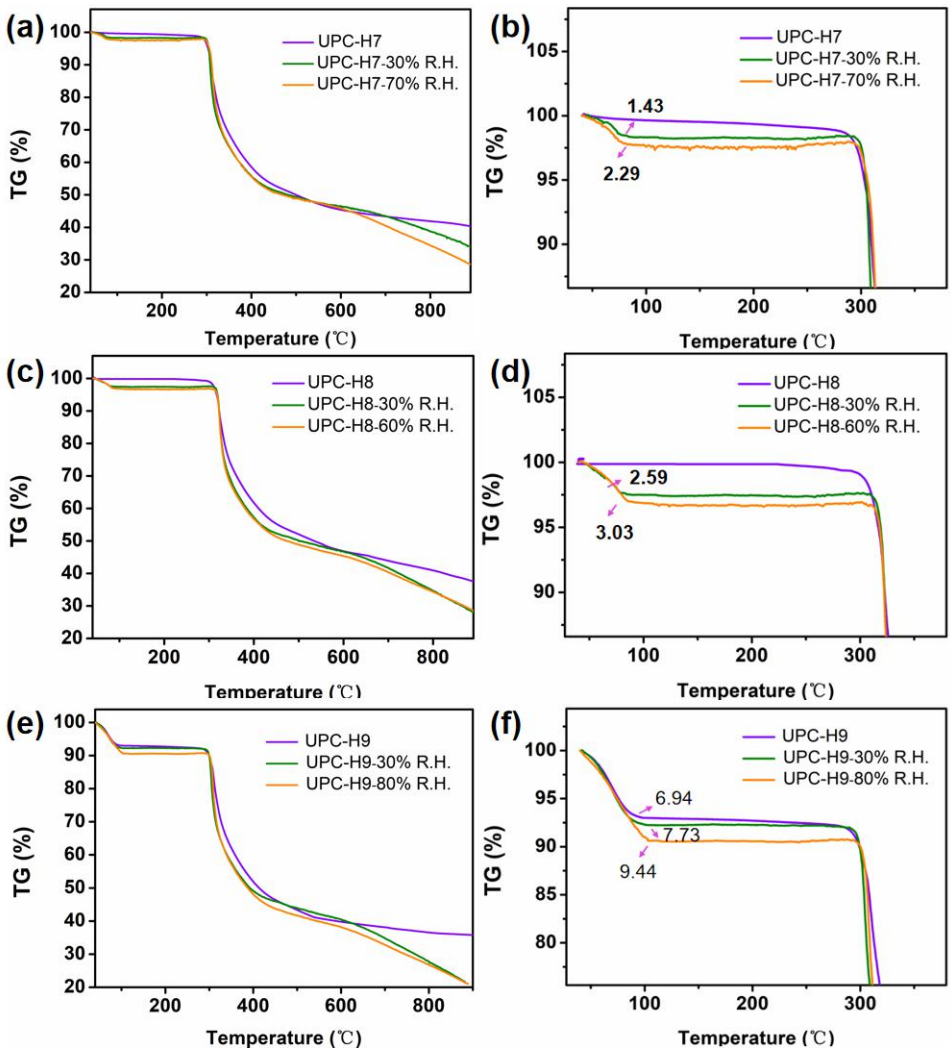

Fig S2 TGA curves of UPC-H7, UPC-H7-30% RH and UPC-H7-70% RH (a), UPC-H8, UPC-H8-30% RH and UPC-H8-60% RH (c), and UPC-H9, UPC-H9-30% RH and UPC-H9-80% RH (e) in the range of 40-900 ºC under N_2 atmosphere; and the local magnification diagram of UPC-H7, UPC-H7-30% RH and UPC-H7-70% RH (b), UPC-H8, UPC-H8-30% RH and UPC-H8-60% RH (d), and UPC-H9, UPC-H9-30% RH and UPC-H9-80% RH (f) showing the weight loss. Note: the samples with humidity was used after standing the pellets for 2 hours at 40 ºC and under 30% RH (UPC-H7-30% RH), at 40 ºC and under 70% RH (UPC-H7-70% RH); at 80 ºC and under 30% RH (UPC-H8-30% RH), at 40 ºC and under 60% RH (UPC-H8-60% RH); at 80 ºC and under 30% RH (UPC-H9-30% RH), at 40 ºC and under 80% RH (UPC-H9-80% RH).

Fig. S3 Quality of UPC-H7 pellets at 40 ℃, 0% R.H. (a) ; at 40 ℃, 30% RH (b); at 40 ℃, 0% RH (c); at 40 ℃, 70% RH (d); quality of UPC-H8 at 80 ℃, 0% RH (e); at 80 ℃, 30% RH (f); at 80 ℃, 0% RH (g); at 80 ℃, 60% RH (h); and quality of UPC-H9 at 80 ℃, 0% RH (i); at 80 ℃, 30% RH (j); at 80 ℃, 0% RH (k); 80 ℃, 80% RH (l). Note: the quality at 0% RH was obtained by weighing immediately after taking the pellet out of the vacuum drying oven, and the quality at other humidity was obtained by weighing immediately after standing the pellets for 2 hours under the related humidity and temperature.

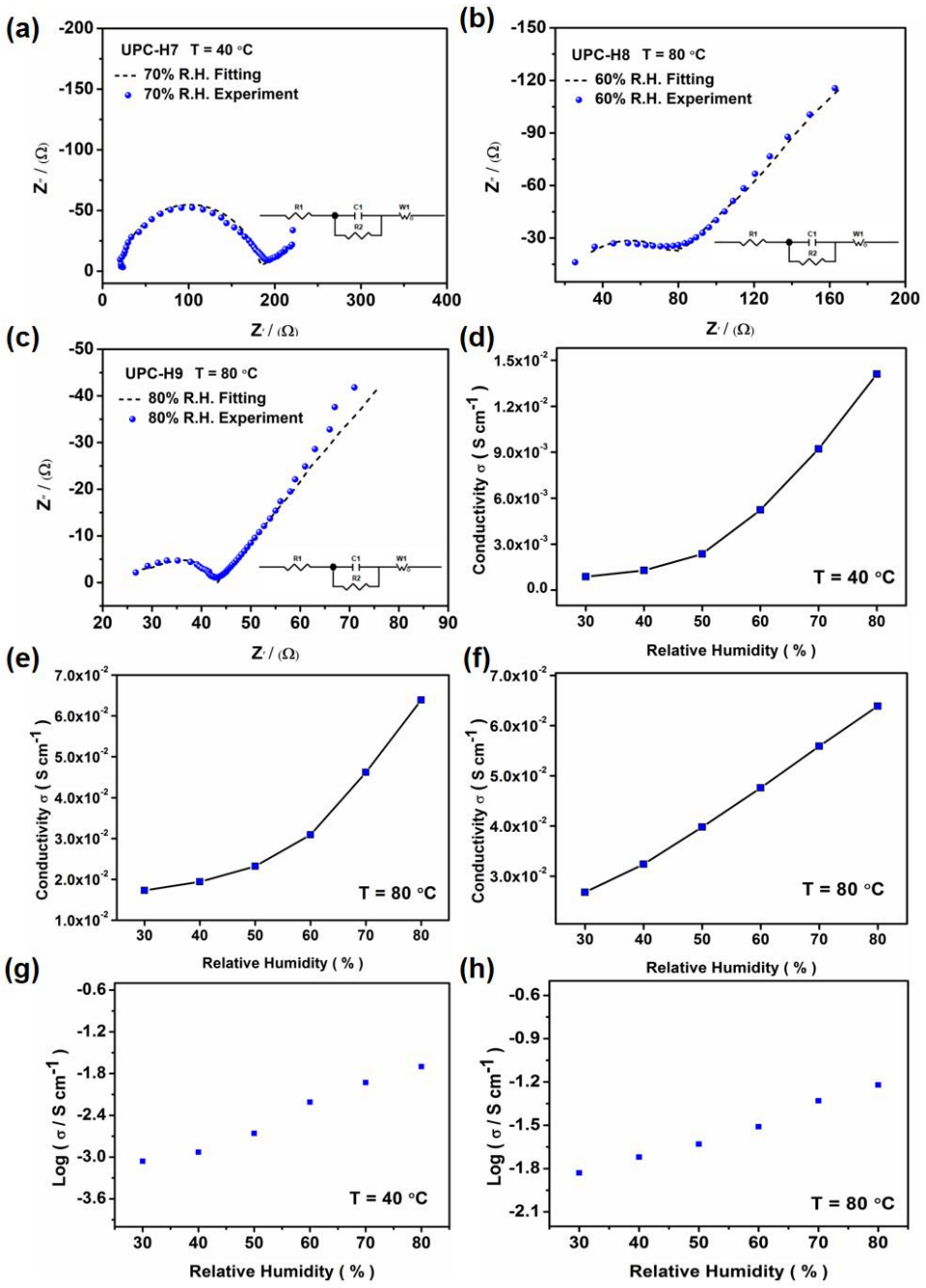

Fig. S4 The experimental Nyquist plot together with the fit lines of UPC-H7 at 40 ºC and under 70% RH (a), UPC-H8 at 80 ºC and under 60% RH, and UPC-H9 at 80 ºC and under 60% RH (c); Proton conductivity of UPC-H7 (30%-70% RH) and UPC-H9 (80% RH) at 80 ºC (d); UPC-H8 (30%-60% RH) and UPC-H9 (70%-80% RH) at 80 ºC (e), and UPC-H9 (30%-80% RH) (f); Log-scaled proton conductivities of UPC-H7 in the range of 30 to 80 R.H. at 40 °C (k), and UPC-H8 in the range of 30 to 80 R.H. at 80 °C (l).

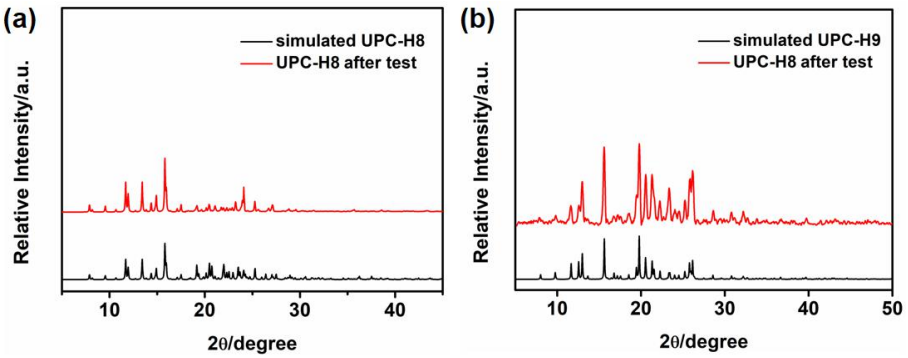

Fig. S5 (a) PXRD pattern of UPC-H8 after testing proton conductivity at 80 ºC and 30%-60% RH; (b) PXRD pattern showing the SCSC transformation from UPC-H8 to UPC-H9 after testing proton conductivity at 80 ºC and 70%-80% RH.

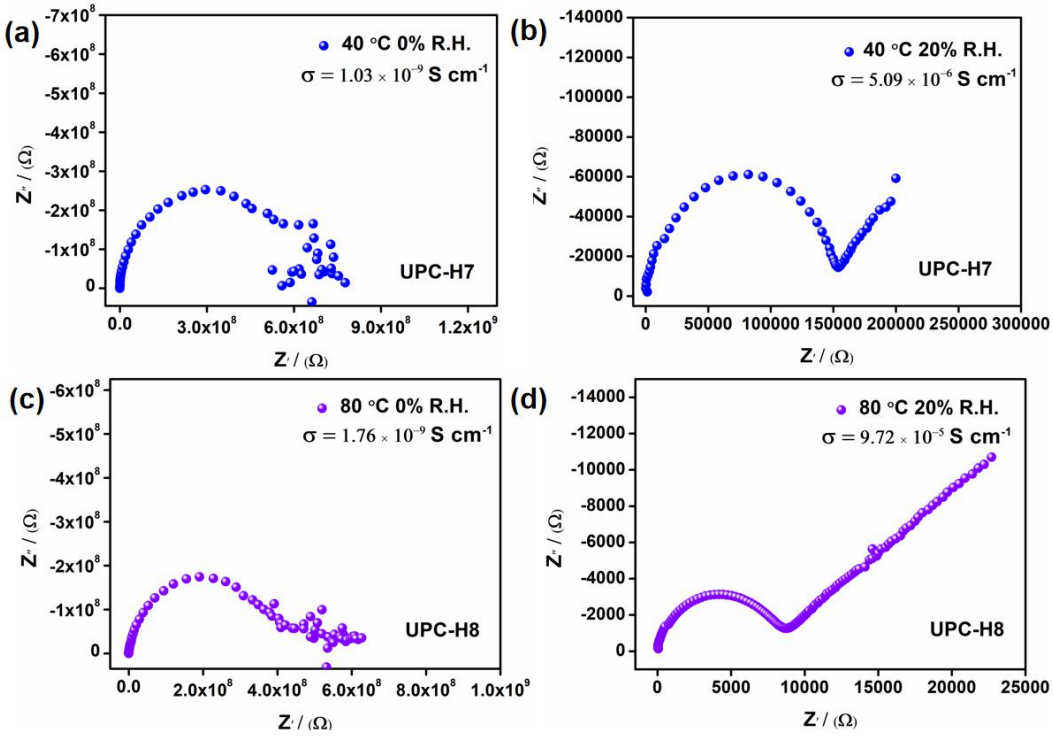

Fig. S6 Nyquist plots of UPC-H7 at 40 °C under 0% RH (a) and under 20% RH (b); (b) Nyquist plots of UPC-H8 at 80 °C under 0% RH (a) and under 20% RH (b). Note: The impedance tests at 0% RH were performed immediately in the humidity chamber with the test temperature but no humidity control after taking the pellet out of the vacuum drying oven with the same temperature as the proton conduction tests.

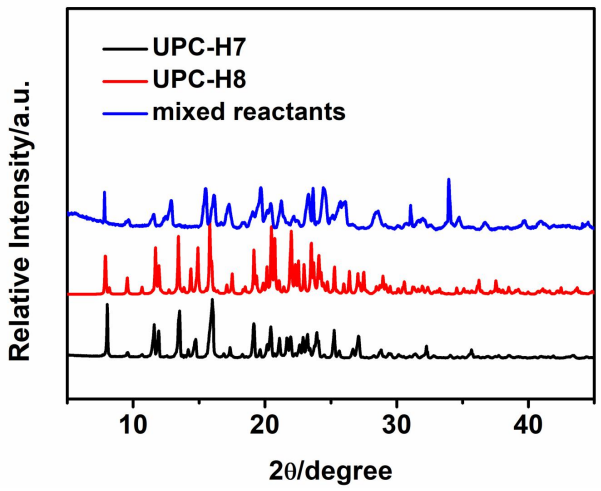

Fig. S7 PXRD pattern of mixed pellets composed of 4,4'-diamino-2,2'-stilbenedisulfonic acid (H_2DAS) and tetramethylammonium hydroxide (TMAOH). Note: H_2DAS and TMAOH were mixed in a molar ratio of 1:2 and slightly ground, then the mixed pellets was pressed using a tableting machine.

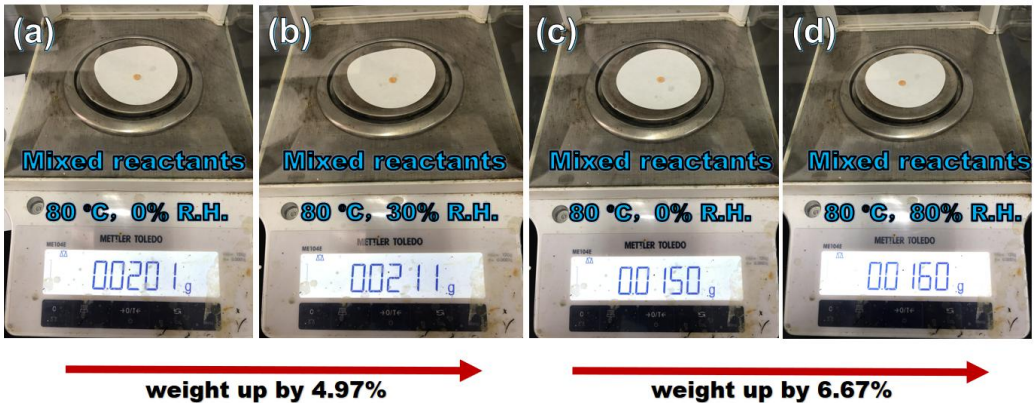

Fig. S8 Quality of mixed pellets composed of 4,4'-diamino-2,2'-stilbenedisulfonic acid (H_2DAS) and tetramethylammonium hydroxide (TMAOH) at 80 ℃ and 0% RH (a); at 80 ℃ and 30% RH (b); at 80 ℃ and 0% RH (c); at 80 ℃ and 80% RH (d). Note: The quality at 0% RH was obtained by weighing immediately after taking the pellet out of the vacuum drying oven, and the quality at other humidity was obtained by weighing immediately after standing the pellets for 2 hours under the related humidity and temperature.

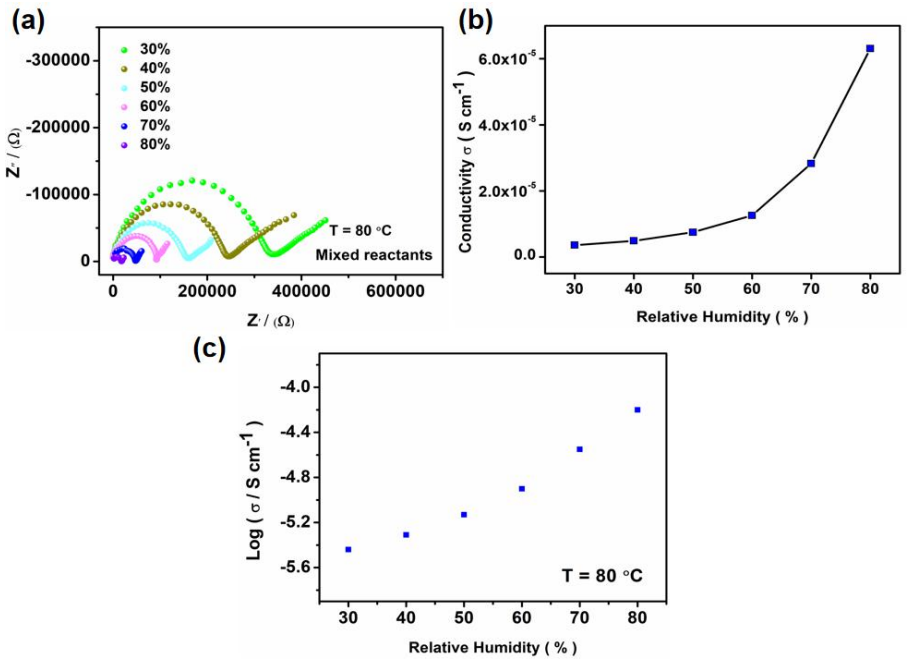

Fig. S9 (a) Nyquist plots, (b) proton conductivity of mixed pellet, and (c) Log-scaled proton conductivities of mixed pellet at 80 °C and under various RH.

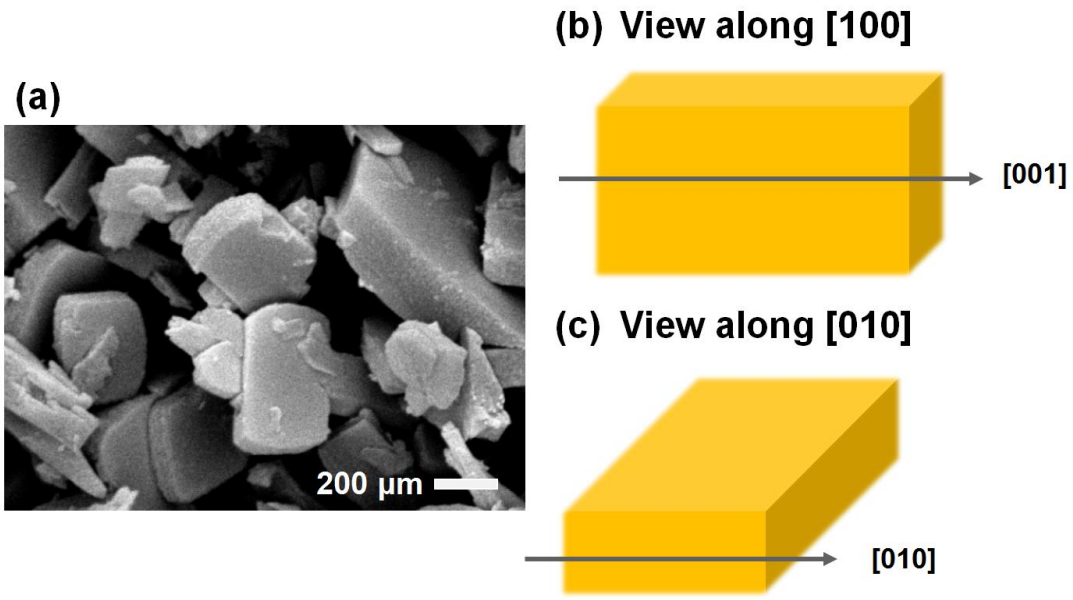

Fig. S10 (a) SEM images of UPC-H8; (b) schematic single crystal viewed along [100]; (c) schematic single crystal viewed along [001] directions.

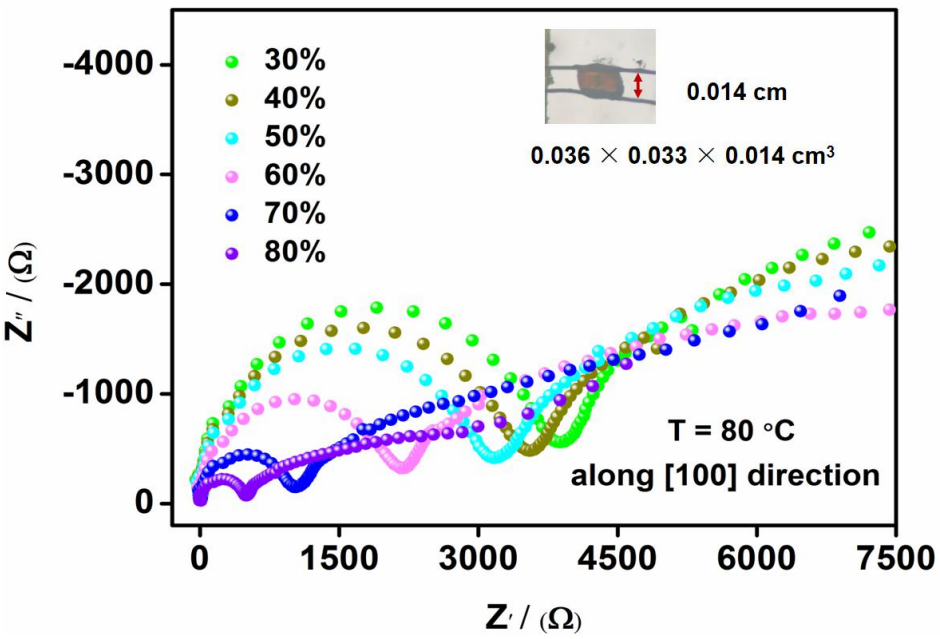

Fig. S11 Nyquist plots for single crystal of UPC-H8 (30%-60% RH) and UPC-H9 (70%-80% R H) along [100] at 80 ºC.

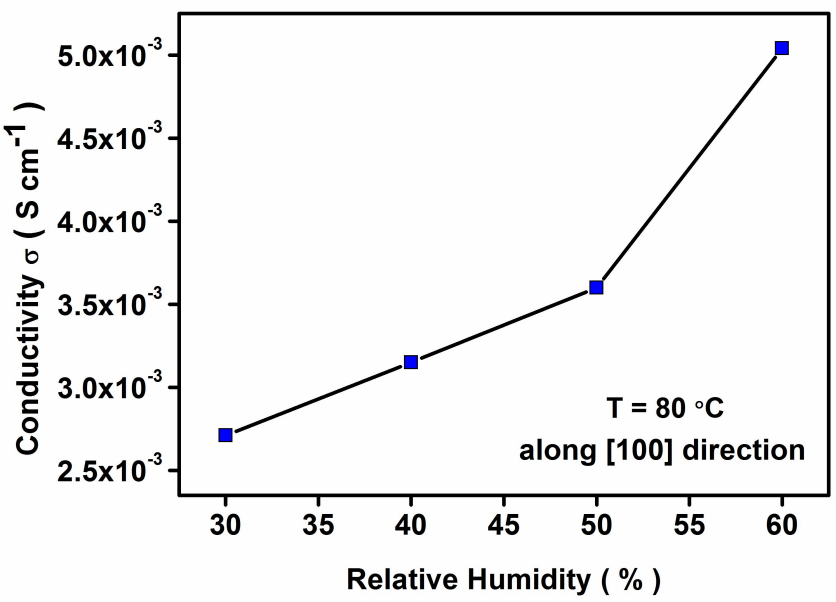

Fig. S12 Proton conductivity for single crystal of UPC-H8 (30%-60% RH) along [100] at 80 ºC.

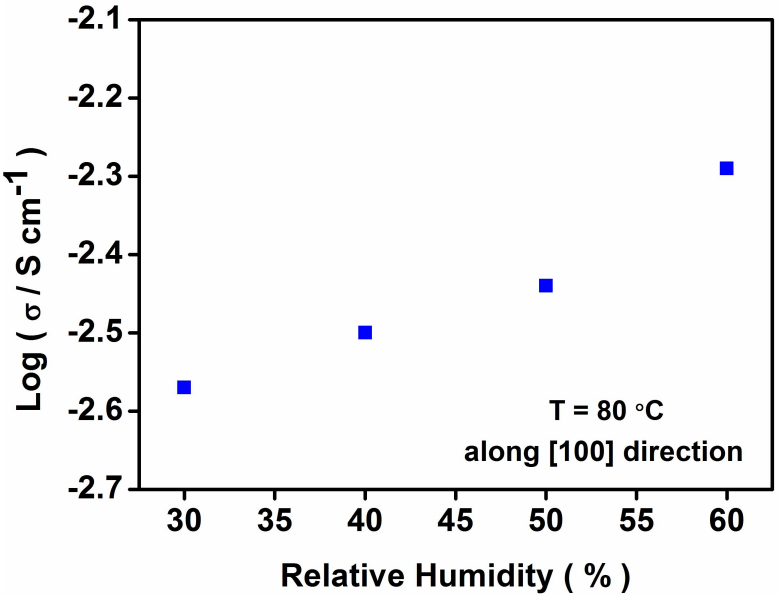

Fig. S13 Log-scaled proton conductivities for single crystal of UPC-H8 (30%-60% RH) along [100] at 80 ºC.

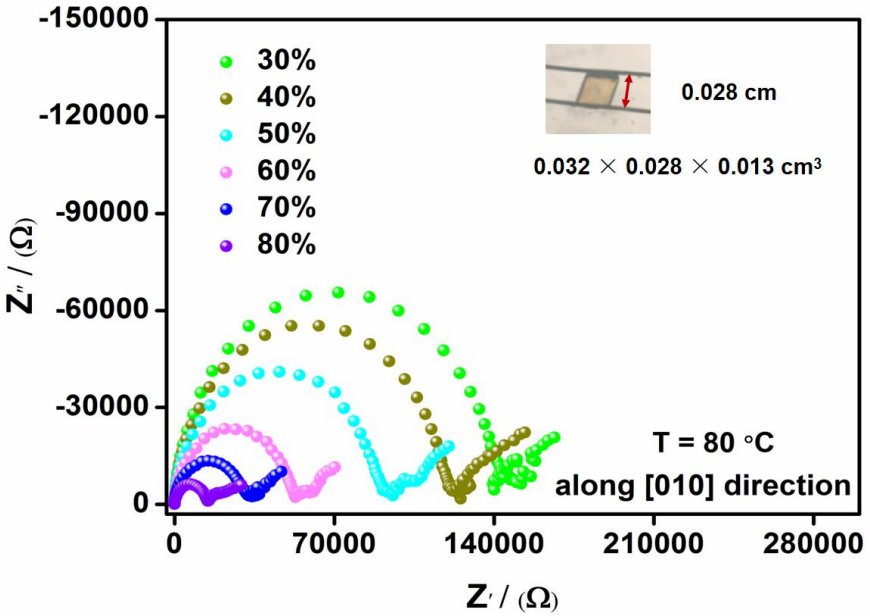

Fig. S14 Nyquist plots for single crystal of UPC-H8 (30%-60% RH) and UPC-H9 (70%-80% RH) along [010] at 80 ºC.

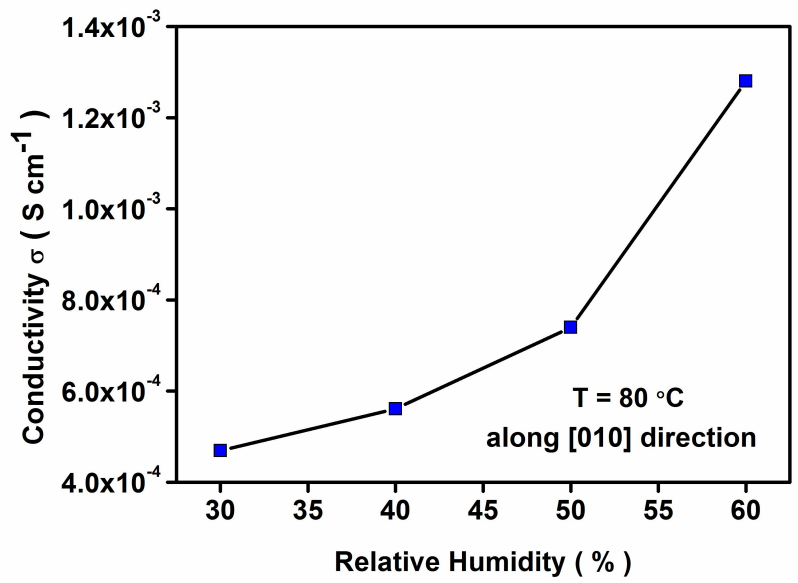

Fig. S15 Proton conductivity for single crystal of UPC-H8 (30%-60% RH) along [010] at 80 ºC.

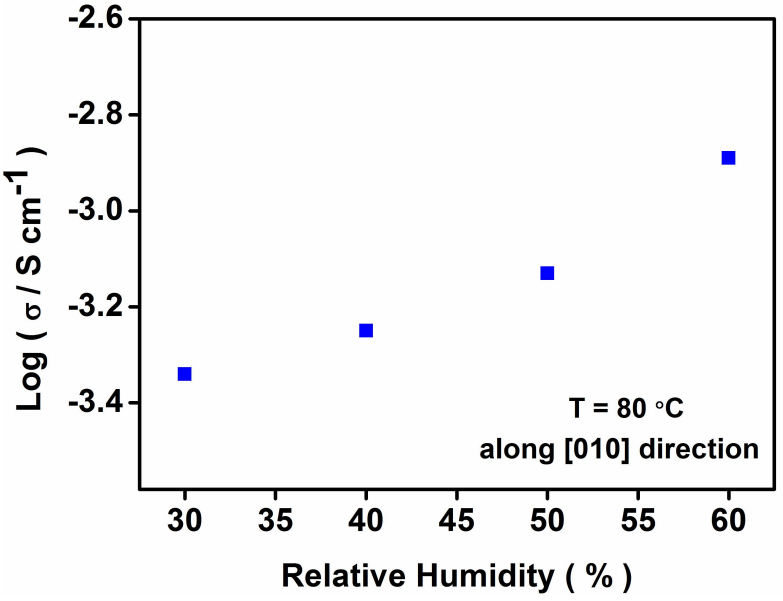

Fig. S16 Log-scaled proton conductivities for single crystal of UPC-H8 (30%-60% RH) along [100] at 80 ºC.

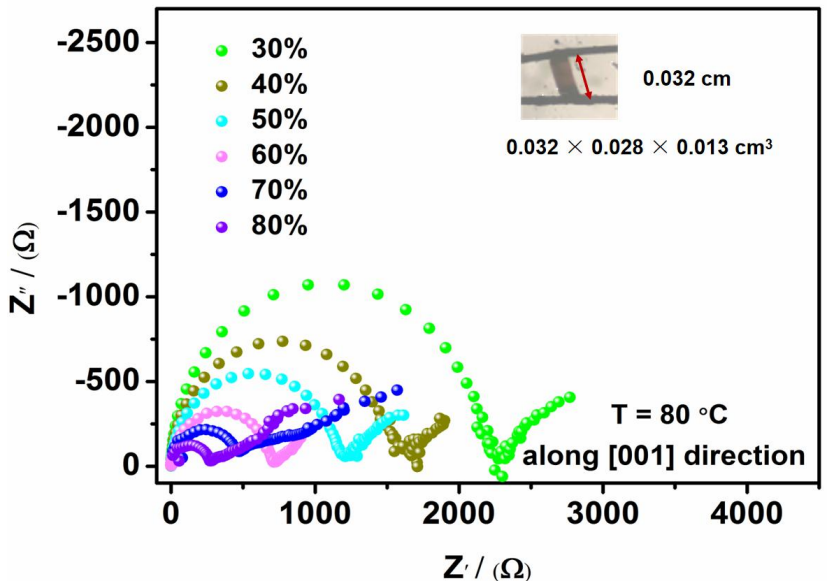

Fig. S17 Nyquist plots for single crystal of UPC-H8 (30%-60% RH) and UPC-H9 (70%-80% RH) along [001] at 80 ºC.

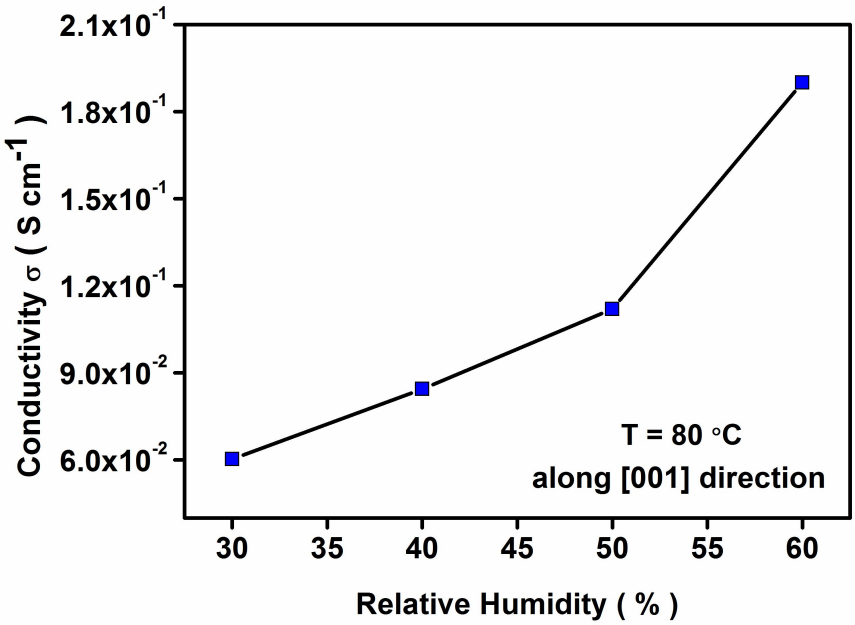

Fig. S18 Proton conductivity for single crystal of UPC-H8 (30%-60% RH) along [001] at 80 ºC.

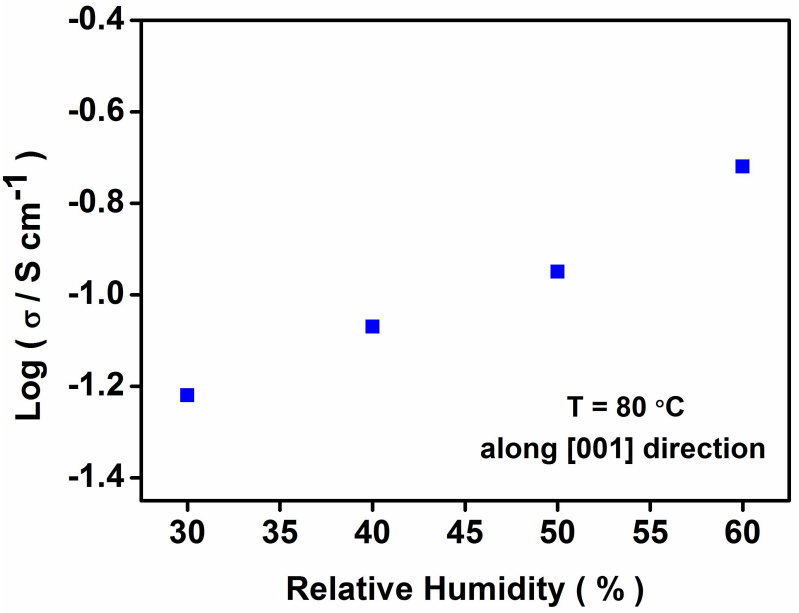

Fig. S19 Log-scaled proton conductivities for single crystal of UPC-H8 (30%-60% RH) along [001] at 80 ºC.

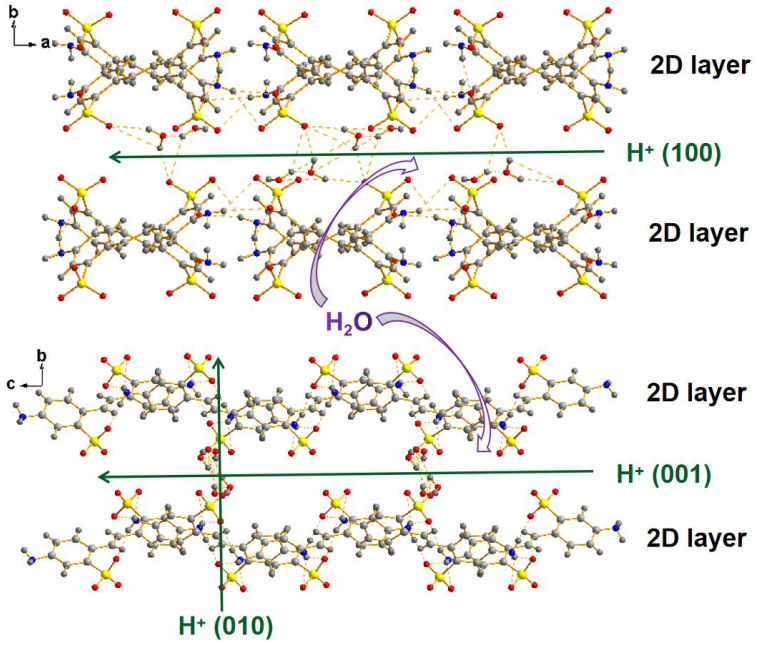

Fig. S20 The possible proton transfer pathways in UPC-H9 along [100] (a), [010] (b) and [001] (c) directions.

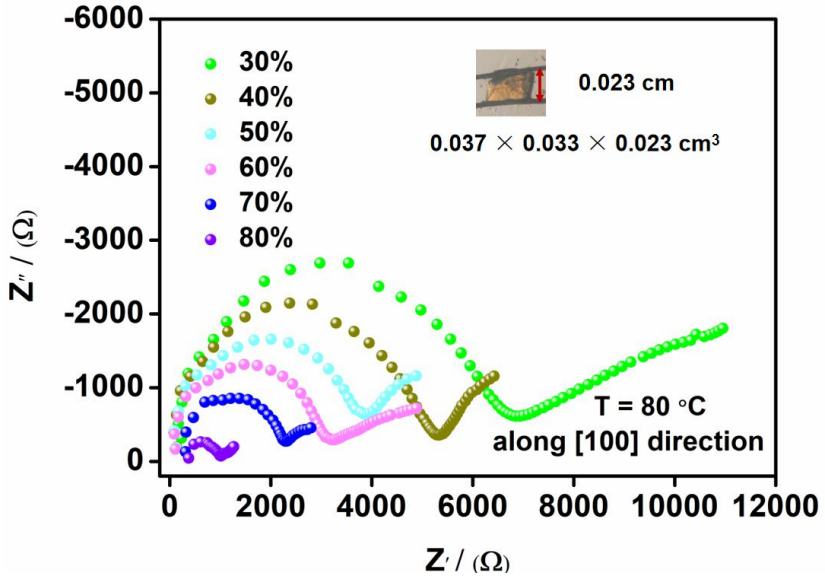

Fig. S21 Nyquist plots for single crystal of UPC-H9 along [100] at 80 ºC and under various RH.

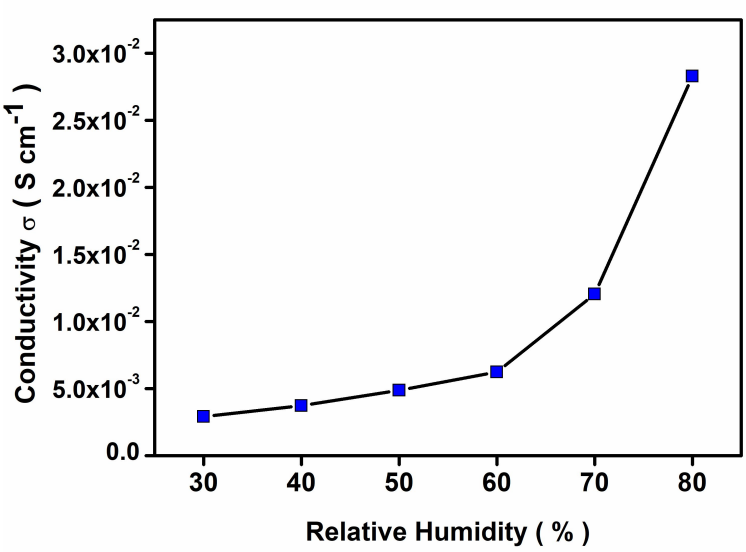

Fig. S22 Proton conductivity for single crystal of UPC-H9 along [100] at 80 ºC and under various RH.

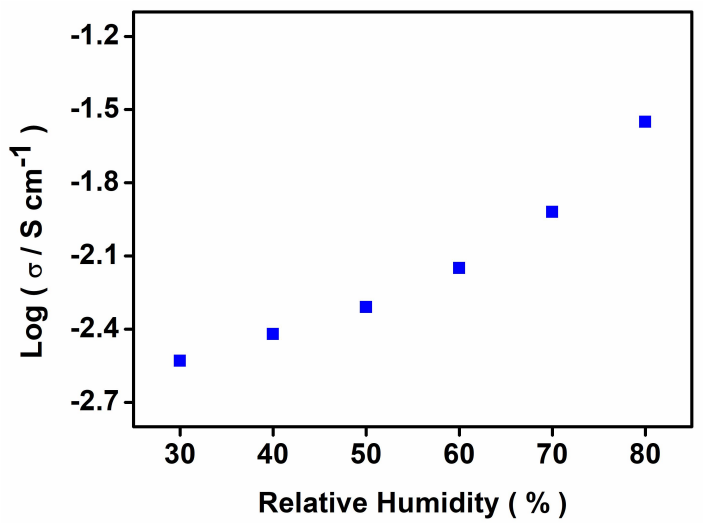

Fig. S23 Log-scaled proton conductivities for single crystal of UPC-H9 along [100] at 80 ºC and under various RH.

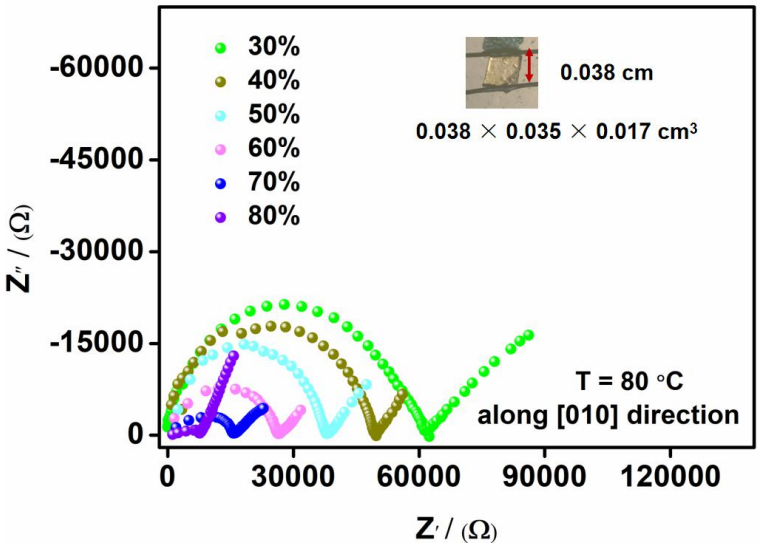

Fig. S24 Nyquist plots for single crystal of UPC-H9 along [010] at 80 ºC and under various RH.

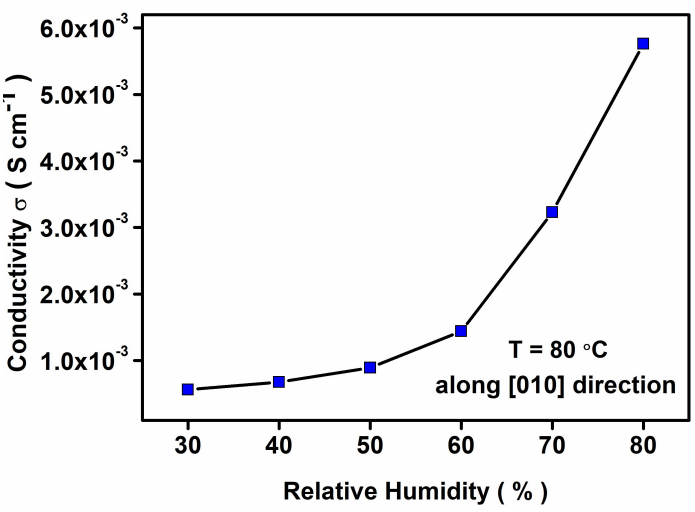

Fig. S25 Proton conductivity for single crystal of UPC-H9 along [010] at 80 ºC and under various RH.

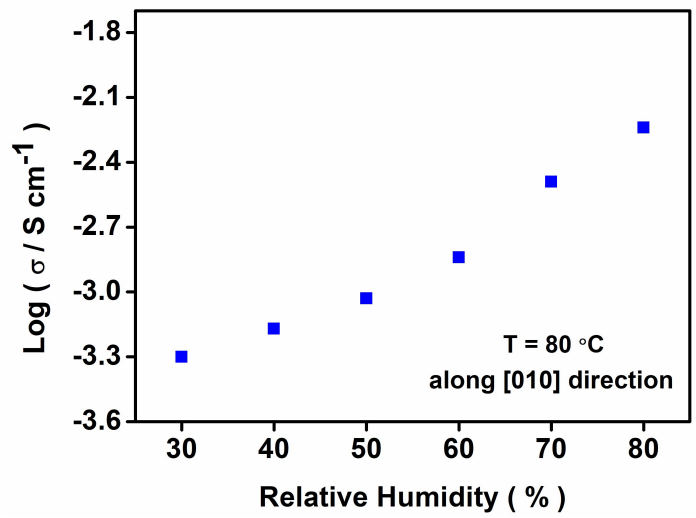

Fig. S26 Log-scaled proton conductivities for single crystal of UPC-H9 along [010] at 80 ºC and under various RH.

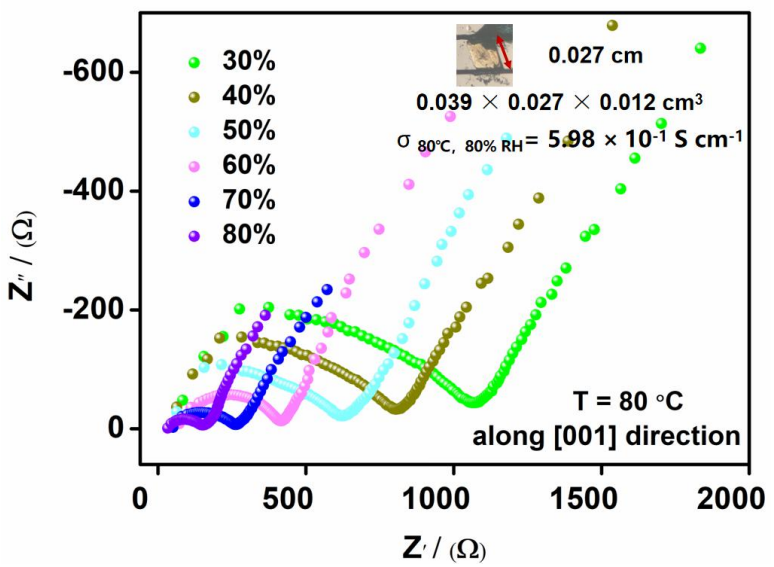

Fig. S27 Nyquist plots for single crystal of UPC-H9 along [001] at 80 ºC and under various RH.

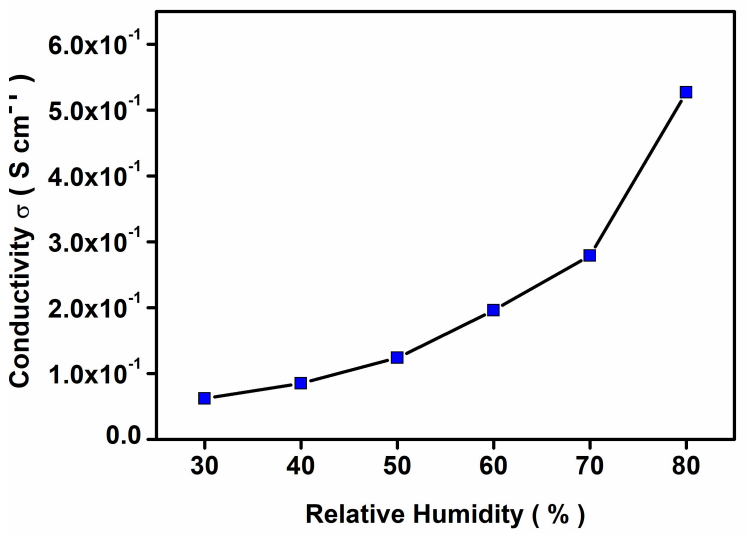

Fig. S28 Proton conductivity for single crystal of UPC-H9 along [001] at 80 ºC and under various RH.

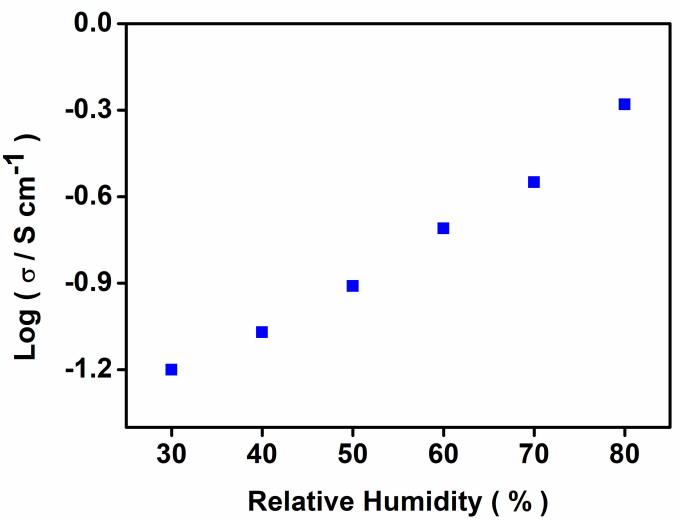

Fig. S29 Log-scaled proton conductivities for single crystal of UPC-H9 along [001] at 80 ºC and under various RH.

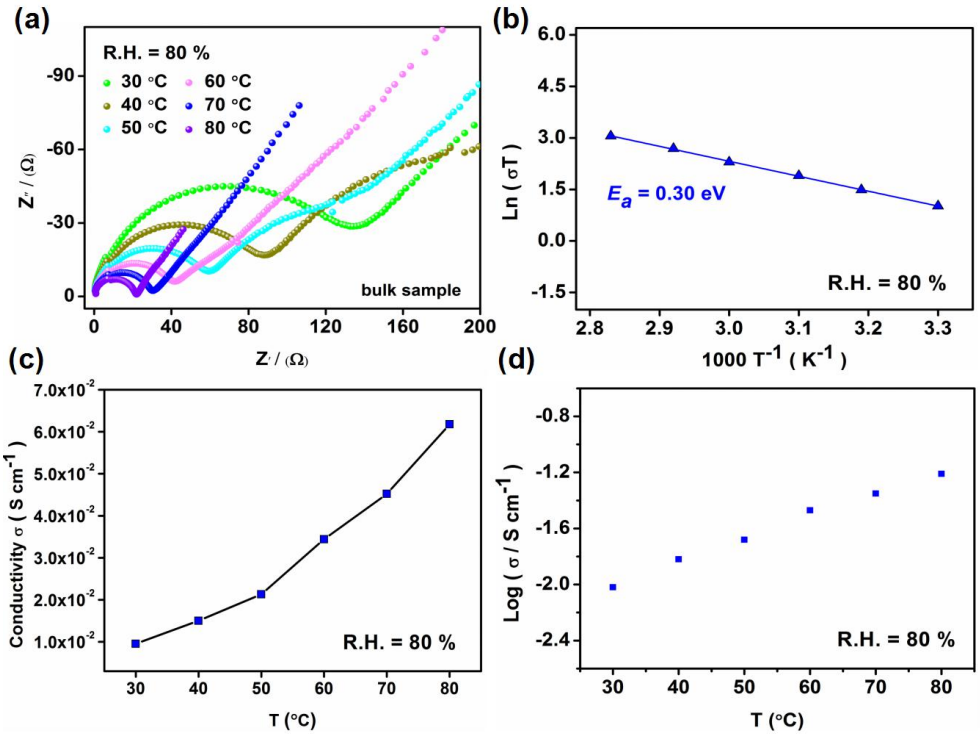

Fig. S30 (a) Nyquist plots, (b) Arrhenius plots, (c) proton conductivities, and (d) Log-scaled proton conductivities of UPC-H9 at 80 ºC under different RH.

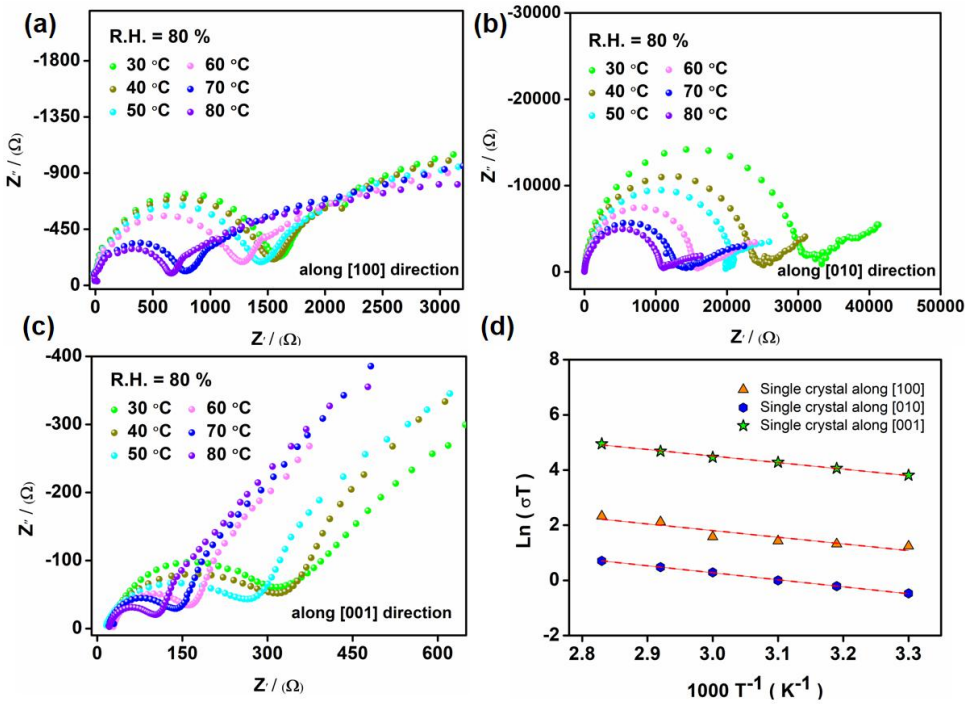

Fig. S31 Nyquist plots for single crystal of UPC-H9 along [100] (a), [010] (b) and [001] (c) under 80% RH and at different temperatures; and Arrhenius plots along [100], [010] (b) and [001] at 80 °C and under 80% RH.

Table S5. Proton conductivities of representative water-mediated complexes under different humidity and at low temperature.

Composition	Conductivity [S cm^{-1}]	Measurement condition	References
UPC-H7	1.28×10^{-3}	40 °C，40 % R.H.	**This work**
UPC-H8	1.73×10^{-2}	80 °C，30 % R.H.	**This work**
UPC-H9	9.52×10^{-3}	30 °C，80 % R.H.	**This work**
UPC-H9	2.68×10^{-2}	80 °C，30 % R.H.	**This work**
{[In(5-Hsip)$_2$(Me_2NH_2)]·DMF·(H_2O)$_{1.4}$}n, PCMOF17	1.17×10^{-3}	25 °C，40 % R.H.	1
VNU-15	7.7×10^{-4}	95 °C，40 % R.H.	2
[(tmen)Pd]$_7$	2.5×10^{-3}	23 °C，75 % R.H.	3
{[(Me_2NH_2)$_3$(SO4)]$_2$[Zn_2(ox)$_3$]}n	1.4×10^{-3}	25 °C，60 % R.H.	4

[Zn(5-sipH)-(bpy)]·DMF·2H_2O	3.9×10^{-4}	25 °C，60 % R.H.	5
PCC-72	3.3×10^{-4}	25 °C，70 % R.H.	6
HOF-GS-11	2.6×10^{-4}	30 °C，60 % R.H.	7
HOF-GS-10	1.78×10^{-4}	30 °C，60 % R.H.	7
{NH(prol)$_3$}[MnCr(ox)$_3$]	1.0×10^{-4}	25 °C，75 % R.H.	8
[NMe_3(CH_2COOH)][FeCr(ox)$_3$]	8.0×10^{-5}	25 °C，65 % R.H.	9
$(NH_4)_4[MnCr_2(ox)_6]\cdot4H_2O$	3.0×10^{-5}	22 °C，65 % R.H.	10
$Co[Cr(CN)_6]_{2/3}\cdot4.8H_2O$	2.9×10^{-5}	22 °C，69 % R.H.	11
[Zn(l-Lcl)(Cl)]·$(H_2O)_2$	1.2×10^{-5}	31 °C，60 % R.H.	12
CB[6]·1.1HCl·11.3H_2O	1.0×10^{-5}	25 °C，70 % R.H.	13
$Eu_2(CO_3)(ox)_2(H_2O)_2\cdot4H_2O$	9.3×10^{-6}	25 °C，40 % R.H.	14
$(NH_4)_2$(adp)[Zn_2(ox)$_3$]·2H_2O	6.0×10^{-6}	25 °C，70 % R.H.	15

References:

1. B. Joarder, J. Lin, G. H. K. Shimizu, Z. Romero, *J. Am. Chem. Soc.* 2017, **139**, 7176.

2. T. N. Tu, N. Q. Phan, T. T. Vu, H. L. Nguyen, K. E. Cordova, H. Furukawa, *J. Mater. Chem. A*, 2016, **4**, 3638.

3. D. Samanta, P. S. Mukherjee, *Chem.-Eur. J.* 2014, **20**, 5649.

4. S. S. Nagarkar, S. M. Unni, A. Sharma, S. Kurungot, S. K. Ghosh. *Angew. Chem., Int. Ed.* 2014, **53**, 2638.

5. P. Ramaswamy, R. Matsuda, W. Kosaka, G. Akiyama, H. J. Jeona, S. Kitagawa, *Chem. Commun.* 2014, **50**, 1144.

6. L. Qin, Y.-Z. Yu, P. -Q. Liao, W. Xue, Z. Zheng, X.-M. Chen, Y.-Z. Zheng, *Adv. Mater.* 2016, **28**, 10772.

7. A. Karmakar, R. Illathvalappil, B. Anothumakkool, A. Sen, P. Samanta, A. V. Desai, S. Kurungot, S. K. Ghosh, *Angew. Chem. Int. Ed.* 2016, **55**, 10667.

8. H. Okawa, A. Shigematsu, M. Sadakiyo, T. Miyagawa, K. Yoneda, M. Ohba, H.

Kitagawa, *J. Am. Chem. Soc.* 2009, **131**, 13516.

9. M. Sadakiyo, H. Okawa, A. Shigematsu, M. Ohba, T. Yamada, H. Kitagawa, *J. Am. Chem. Soc.* 2012, **134**, 5472.

10. E. Pardo, C. Train, G. Gontard, K. Boubekeur, O. Fabelo, H. Liu, B. Dkhil, F. Lloret, K. Nakagawa, H. Tokoro, S. Ohkoshi, M. Verdaguer, *J. Am. Chem. Soc.* 2011, **133**, 15328.

11. S.-I. Ohkoshi, K. Nakagawa, K. Tomono, K. Imoto, Y. Tsunobuchi, H. Tokoro, *J. Am. Chem. Soc.* 2010,**132**, 6620.

12. S. C. Sahoo, T. Kundu, R. Banerjee, *J. Am. Chem. Soc.* 2011, **133**, 17950.

13. M. Yoon, K. Suh, H. Kim, Y. Kim, N. Selvapalam, K. Kim, *Angew. Chem.* 2011, **123**, 8016; Angew. Chem., Int. Ed. 2011, 50, 7870.

14. Q. Tang, Y.-W. Liu, S.-X. Liu, D.-F. He, J. Miao, X.-Q. Wang, G.-C. Yang, Z. Shi, Z. Zheng, *J. Am. Chem. Soc.* 2014, **136**, 12444.

15. M. Sadakiyo, T. Yamada, H. Kitagawa, *J. Am. Chem. Soc.* 2009, **131**, 9906.